PR 1971

"SAFE AND EFFECTIVE STIMULATION OF NERVOUS TISSUE"

Contract No. NO1-NS-5-2324

QUARTERLY PROGRESS REPORT #3
July 1 - Sept 30, 1995

HUNTINGTON MEDICAL RESEARCH INSTITUTES
NEUROLOGICAL RESEARCH LABORATORY
734 Fairmount Avenue
Pasadena, California 91105

W.F. Agnew, Ph.D.
D.B. McCreery, Ph.D.
T.G.H. Yuen, Ph.D.
L.A. Bullara, B.S.
R.R Carter

Introduction and Summary

Prolonged electrical stimulation of a peripheral nerve at moderately high frequency (50 Hz or greater) and at moderately high amplitude will induce a characteristic form of neural injury, in which the myelin surrounding the axons collapses into the axonal space. This type of damage is most conspicuous approximately 7 days after the session of electrical stimulation, and at this stage, it is designated Early Axonal Degeneration (EAD). One cardinal feature of EAD is that only a small fraction of the large axons are unequivocally affected, and the majority of the axons appear to be normal.

In this report, we describe a computerized morphometric system that was used to quantify stimulation-induced injury in peripheral nerves. A preliminary report of these procedures and results were presented in our Quarterly Report #11, (Contract No. NO1-NS-2-2323) .

The procedure is a 2-phase process, with the image analysis implemented via a commercial image analysis program (Global Lab Image, Data Translation, Inc), followed by an analysis and editing, using custom software, of the morphometric parameters of each object identified by the Global lab Image program. Both phases of the analysis are implemented on IBM-compatible personal computers. The custom software counts the number of axons undergoing EAD, based on the criteria for the range of myelin cross-sectional area and axonal cross- sectional area from normal (unstimulated) nerves. The correlation between the normalized stimulus amplitude and the number of degenerating axons is the same as when the analysis is performed by an experienced histopathologist (R=0.86) and carries the advantage of being entirely objective.

We also demonstrated that axons of intermediate size (4.8 to 9 μm in diameter) are most vulnerable to stimulation-induced injury. This has certain implications regarding the mechanism underlying the stimulation-induced injury.

Finally, we used the morphometric analysis to demonstrate that by 5 to 13 weeks after a session of damaging stimulation, the nerve contains few if any hypomyelinated axons. This indicates that the distal segments of axons damaged by the electrical stimulation do not subsequently regenerate, or that at the very least, the process of

regeneration is greatly prolonged, when compared to the rate of regeneration following localized mechanical trauma.

We also present preliminary results from a similar morphometric analysis of stimulation-induced changes in neurons in the cat cerebral cortex. The stimulation-induced changes in the cortex were quantified as difference in the geometric sum of two morphometric indices, one quantifying the shape of the neurons in the histologic section and one quantifying the optical density of the neurons (their affinity for the histologic stain). These data indicate that a computer-assisted morphometric analysis can add a useful dimension to our studies of stimulation-induced neuronal damage in the CNS, especially in situations requiring quantitation of changes in small populations of neurons (for example, a dose-response study of the effect of microstimulation on the neurons surrounding the microelectrode's active site).

METHODS

Morphometric analysis of stimulation-induced injury in peripheral nerve.

The HMRI bidirectional helical stimulating electrode array was used in this study. The stimulating electrodes were implanted around both sciatic nerves of adult cats of either sex. A pair of recording electrodes is implanted subcutaneously over the lumbosacral spinal cord to record the compound action potentials evoked in the sciatic nerve by the stimulating electrode. One recording electrode is implanted at approximately the L5 level, and the other member of the pair is implanted approximately 5 cm caudally. With this arrangement, the compound action potentials evoked in the left or right nerve can be recorded with a single pair of recording electrodes, and there will be no danger of inflicting additional mechanical trauma upon the nerve or nerve roots.

Three weeks or more after implantation of the electrodes, the cats were anesthetized with Propofol and both nerves were stimulated continuously for 8 hours. The stimulus waveform was a charge-balanced, controlled-current, biphasic pulse pair. Each phase of the biphasic pair is 100 μsec in duration, with a 400 μsec delay between the first and second phases. This waveform excites both large and small axons in the nerve (Gorman and Mortimer 1983, McCreery et al 1992, van der Honert and Mortimer 1979).

Prior to the start of the 8 hours of continuous stimulation, we measured the recruitment characteristics of the Averaged evoked Compound Action Potential (AECAP), the response evoked by the stimulating electrodes and recorded over the spinal cord. In the peripheral nerve of the cat the first large component of the AECAP (the α component) represents the activity in the alpha and gamma efferent axons and the large afferent axons. To determine the recruitment characteristics of α component of the AECAP, the nerve is stimulated at each of several amplitudes, and the amplitude of the α component is plotted against the stimulus pulse amplitude. In addition, five unstimulated nerves were included in the study.

The sciatic nerves were prepared for histologic examination, as described in previous Quarterly reports and publications. The nerves were resected from the leg and embedded in plastic (Polysciences Polybed), cut to a thickness of 1 μm. The myelin was stained with osmium, and the endoneurium and axoplasm was counter-stained with methylene Blue.

For each nerve, 12 microscopic fields, each spanning approximately 186 x 180 μm, were scanned into the computer, using a high-resolution CCD camera (1024 x 972 pixels, and 256 grey levels). Each digitized image was then analyzed using a commercial image analysis program (Global Lab Image, from Data Translation, Inc). This program can identify objects within the field of the digitized image. For each field, the operator must specify a grey level (brightness), by which the GLI software establishes the boundary between the object and the surrounding background. The histograms of the grey levels of the approximately 1,000,000 pixels forming the image is computed by the GLI software, and then analyzed by a custom software utility. The histogram contains 3 peaks, representing the myelin (darkest), the endoneurium surround the myelin, (lighter) and the axoplasm (lightest). A typical histogram is shown in Figure 1. The custom software deconvolves the peaks, and identifies the grey level that is brighter than 97.5% of the myelin. This grey level is then used to obtain the optimal differentiation between the myelin and the surrounding endoneurium.

Eleven morphometric parameters were computed for each object, including total area, area of included holes, roundness (circularity) and average brightness. The tabulated parameter files were then edited and analyzed with the aid of a custom software program in order to remove artifact objects and joined objects, and all objects having a total cross sectional area less than 10 μm^2 (small myelinated axons cannot be identified reliably by the image analysis program, due to their low and variable contrast against the surrounding endoneurium).The number of fibers undergoing early axonal degeneration was also counted automatically, using criteria established from the morphometric analysis of unstimulated nerves.

Morphometric analysis of cerebral cortical neurons

The feasibility of using automatic morphometry to quantify the stimulation-induced changes in neurons was evaluated in tissue subjacent to electrodes implanted on the cortical surface, and also from one animal that had been implanted with penetrating activated iridium microelectrodes 3 weeks previously. In both cases, the 7 hours of continuous stimulation (charge-balanced, controlled current, pulse pairs) was conducted with the animals lightly anesthetized with Nembutal (Pentobarbital). Immediately after the end of the stimulation,. The animals were anesthetized with Surital and a brief saline rinse perfused through the ascending aorta, followed by 2L of Karnovsky's fixative.

Following perfusion, the head with brain and array(s) in situ, were left in fixative until autopsy the following day. At autopsy the electrodes were removed, tissue blocks resected, Imbedded in paraffin and stained with Nissl (for assessment of neural elements) or Hematoxylin and Eosin (H&E). The histologic sections were then photographed directly into the computer, using the high-resolution CCD camera described above.

RESULTS

I: Morphometric analysis of peripheral nerve

Prolonged electrical stimulation of a peripheral nerve at moderately high frequency (50 Hz or greater) and at moderately high amplitude will induce a characteristic form of neural injury, in which the myelin surrounding some of the axons collapses into the axonal space. This type of damage is most conspicuous approximately 7 days after the session of electrical stimulation, and at this stage, it is designated Early Axonal degeneration (EAD). Later, axons undergoing EAD degenerate completely, and the remnants of the axoplasm and myelin are phagocytized by macrophages (Agnew et al, 1990a). Figure 2A shows a cross-section of part of a cat sciatic nerve, in which several of the myelinated axons are undergoing EAD (Arrows) . The cardinal feature of EAD is that the cross-sectional area of the axoplasm is much reduced, so that a disproportionate part of the

cross-section is occupied by myelin. In some cases, the myelin buckles and actually intrudes into the axon, and when the axon is viewed in cross-section, the "redundant myelin" may lie within the profile of the axon. Thus, during EAD, the cross-section of the axoplasm is reduced, while the cross-section of the myelin remains constant or increases. These morphologic changes form the bases of our computerized analysis of stimulation-induced injury in peripheral nerve.

Figure 2B shows a scatter plot of cross-sectional axonal area vs. Cross-sectional myelin area for 2408 myelinated axons from an unstimulated cat sciatic nerve. Each point represents one myelinated fiber. As noted previously, only axons with total cross-section areas greater than 300 pixels^2 (10 μm^2) are considered. Both axes are logarithmic, and the considerable variation in myelin area for a particular axonal area is apparent. This phenomenon has been noted by other authors. The axonal diameters listed to the right of the ordinate correspond to the diameters of circular axonal profiles with the corresponding areas. In fact, most axonal profiles are quite irregular, so these values are only approximate. The plot of myelin area vs. axonal area contains the same information as the more familiar plot of g-ratio (equivalent fiber diameter/equivalent axon diameter) vs. equivalent axonal area. However there may be severe distortion of the profiles of the axons undergoing EAD, so the scatter plot of myelin area vs. axonal area was judged to be more descriptive of the pathological process. It is notable that the ratio of the myelin and axon areas is unaffected by some common sources of artifact, including the quite common situation in which the fibers are sectioned somewhat obliquely, as occurs when they do not run precisely perpendicular to the plane of the histologic section. However, the g-ratio for each point (fiber) can be calculated as $(A/(A+M)^{.5}$, where A and M are the axonal and myelin areas, respectively. Figure 2C is the plot of g-ratio vs. axonal area, for the unstimulated nerve.

The cluster of points in Figure 2B is bounded by two lines. The lower line is described by the relation [myelin area - 5.8 μm^2 = 5 x Axon area] and was selected so that only 0.01% of the axons from 5 control nerves lie below it. The portion of the plot below the line represents a region in which there is excessive myelin. This is designated as the

region of shrunken axonal profiles, or SAP region. The few profiles from normal nerves that lie within the SAP region are due to fibers that were sectioned immediately adjacent to a node of Ranvier, a location at which the axonal profile is greatly reduced. The upper line in Figure 2B , [myelin Area =.67 x Axon Area] was selected to lie above all of the axons in a normal nerve. The portion of the plot above this line represents a region in which the myelin is abnormally thin (hypomyelinated axons) as occurs when an axon attempts to regenerate its distal segment after sustaining mechanical trauma. The hypomyelination line corresponds to a g-ratio of 0.79, which has been shown in other morphometric studies of peripheral nerves to be close to the upper limit for normal myelinated axons (Touch et al, 1989)

Figure 3A and 3B show scatter plots of the fibers from two nerves that had been quite heavily damaged by 8 hours of continuous electrical stimulation. Eleven percent, and 5.2% of the axons, respectively, are in the SAP region, and are thus considered to be undergoing EAD. The nerve depicted in Figure 3A was stimulated at 100 Hz, and represents the highest percentage of EAD seen in any of the nerves examined. The degree of damage depicted in Figure 3b is more typical of that inflicted by 8 hours of continuous stimulation at 50 Hz.

Figure 4 shows a plot of the amplitude of the electrical stimulus (abscissa) vs the % of axons within the SAP region, for 18 cat sciatic nerves stimulated for 8 hours at 50 Hz, and sacrificed 7 days later. We have shown previously that in order to obtain a good correlation between stimulus amplitude and stimulation-induced damage in peripheral nerve, the stimulus amplitude must be normalized on the current needed to fully recruit the earliest (α) component of the compound action potential induced by the stimulation; the correlation between neural damage and stimulus amplitude is poor when the stimulus is expressed simply as charge per phase or as current (McCreery et al, 1992). The correlation between the percentage of axons in the SAP region, and the normalized stimulus intensity is 0.86, which is virtually the same as when the EAD are counted manually (0.87), using subjective criteria for EAD (McCreery et al, 1995). R^2 can be interpreted as the "conditional variance", that is, the percentage of the total variance that

can be attributed to the stimulus (Afifi and Azen, 1972) Here, R^2 = 0.75 (75%). The remaining minority contributions to the variance between nerves and between animals must be attributed to other variables that were not controlled in this study. Thus, the accuracy of the automated morphometric analysis of the neural damage is comparable to that of a trained neuropathologist, and carries the advantage that the criteria for damage can be defined quantitatively and unambiguously.

The 2-phase automated procedure using custom software for the final morphometric analysis is very flexible. For example, it is possible to determine the caliber of the myelinated axons that are most vulnerable to stimulation-induced neural damage. The range of myelin cross-sectional area was partitioned into bands 400 pixels (13 μm^2) in width. For each band, the percentage of the axons within the SAP region was calculated. This was done for 3 nerves in which enough axons were damaged so that at least 5 axons within each band were in the SAP region. Figure 5 shows that the highest proportion of damaged axons were those with myelin areas of 30 to 60 μm^2. Figure 6 depicts the cluster of fibers from the unstimulated nerve shown in Figure 2B, with the locations of the upper and lower ranges of the three peaks depicted in Figure 5 represented as vertical lines. The corresponding range of axonal cross sectional areas are indicated on the ordinate. The most vulnerable axons had (equivalent axon diameters) of approximately 4.8 to 9 μm, prior to being damaged. This model assumes that the cross-sectional area of the myelin does not change substantially as the axons became damaged (in Figure 3A and 3B, the points within the SAP region are assumed to have originated from directly above). However, in some cases, the myelin actually intrudes into the axon during the injury process, and when the awxons are viewed in cross- section, this results in the phenomenon of "redundant myelin" in which the cross-sectional area of the myelin may actually increase. This will cause the model to slightly overestimate the caliber of the fibers that are most vulnerable to damage. In any event, the largest axons are relatively immune to stimulation-induced injury. In the cat sciatic nerve, the most numerous fibers with axonal diameters of 5 to 9 μm are the axons of the alpha motoneurons and the group II afferents. The largest fibers in the nerve, which are relatively refractory to the stimulation-induced

injury, are primarily group I-A afferents from the muscle spindle primary endings and the Golgi tendon organs.

The relatively high vulnerability of the medium-sized axons to stimulation-induced injury, and the relative immunity of the largest axons has certain implications regarding the mechanism underlying the damage, and in particular, support our hypothesis that the injury is "excitotoxic" in origin. In support of this hypothesis is our earlier finding that blocking the action potentials with a local anesthetic will protect the nerve from stimulation-induced injury (Agnew et al, 1990ab). One difficulty with the argument that the injury is due to the stimulation-induced neuronal excitation is that the threshold current of the damage is higher than the activation threshold of the axons that are damaged. This has led us to hypothesize that the damage is due to a "mass-action" phenomenon, in which axons that are vulnerable to metabolic stress are injured when a sufficient proportion of the total complement of both large and small axons is excited by the stimulus, such that there is a deleterious change in the extra-axonal environment (For example, a prolonged elevation of extraaxonal potassium). An alternate hypothesis is that the injury is due to electroporatation of the axonal membranes by the applied stimulation field. However, it is difficult to reconcile the hypothesis that the injury is due to membrane electroporation with the findings of the local anesthetic experiments described above. The present results also argue against electroporation as the primary cause of the injury. Experimental measurements as well as mathematical analyses based on the Frankenhauser-Huxley model show that the largest axons would undergo the greatest electrotonic depolarization and repolarization (Rattay 1989, Rubenstein, 1991). Therefore, if membrane electroporation were the mechanism that is primarily responsible for the stimulation-induced damage, the largest fibers should sustain the greatest injury,. It may be significant that the group II axons are also the most vulnerable to injury from diabetic neuropathy (Kanda, 1984). In this disorder, the axonal pathology may be secondary to the degenerative changes in the nerve's microcirculation, resulting in decreased endoneurial blood flow (Dyck, 1989). If the stimulation-induced injury is indeed caused by uncompensated changes in the extraaxonal environment, then some patients, notably

those whose microcirculation is compromised, are likely to be more vulnerable to such injury. Extra care may be needed when such individuals are considered for FES applications.

We also addressed the question of whether axons damaged by electrical stimulation are subsequently able to regenerate. We have shown that at least some of the axons undergoing EAD will subsequently degenerates (Agnew et al 1990b). When myelinated axons in a peripheral nerve do regenerate after trauma, their myelin sheaths remain abnormally thin (high g-ratio). Figure 7A shows a portion of a small fascicle of an unstimulated cat sciatic nerve that had sustained injury from a poorly fitting electrode array. The animal was sacrificed approximately 16 weeks after implantation of the array. The damaged region contains scar tissue and some thinly-myelinated fibers which have begun to regenerate. Figure 7B shows the scatter plot of myelin area vs axon area for this region. The cluster is much more dispersed than for the control nerve (Figure 2B) and the hypomyelinated axons lie on or above the line delimiting the region of hypomyelination . At this stage, there is little or no evidence of ongoing EAD, indicating that virtually all of the damage occurred at an earlier time.

Figure 8A shows a scatter plots of a nerve from a cat sacrificed 5 weeks after 8 hours of electrical stimulation at an intensity that would have been expected to damage approximately 4% of the myelinated axons, based on the regression line shown in Figure 4. By 5 weeks after the damaging stimulation, a few points are still within the SAP region of the plot, indicating ongoing EAD, but none are above the main cluster or within the region of hypomyelination, indicating that none of the damaged fibers had begun to regenerate. Figure 8B shows the scatter plot from a nerve that received a similarly damaging stimulation and was sacrificed 13 weeks later. At this time, 8 of the 1856 axons in the sample were undergoing EAD. Two or three other points are close to the hypomyelination line, and may represent regenerating axons. However, the latter constitute only a small percentage (0.01%) of the axons that should have been damaged by the stimulation (~4%). This indicates that most of the axons damaged by the electrical

stimulation have disappeared and do not regenerate, or at least that their regeneration is greatly delayed.

II. Morphometric analysis of stimulation-induced changes in cortical neurons

We have also begun to develop a morphometric analysis of the effects of prolonged microstimulaiton on the neurons of the cerebral cortex. From a technical standpoint, this has proven to be a more difficult problem than has the analysis of the peripheral nerve, since the contrast between the neurons and the surrounding neuropil is considerably less than that of myelin against the axoplasm and endoneurium. This exacerbates the problem of delimiting objects based on their gray-scale difference from their surrounding, and each neuron must be processed individually. However, since only a few neurons lie close to each active site on a penetrating microelectrode, this is not seen as a prohibitive difficulty. Figure 9A shows a field of normal neurons in the parietal cerebral cortex of a cat (Nissl stain). Figure 9B and 9C show neurons subjacent to electrodes on the surface of the cerebral cortex. The electrodes in Figure 9B were judged by a neuropathologist (T.G.H.Y.) To be more severely affected by the electrical stimulation than were the neurons shown in Figure 9C. As is evident in Figure 9, when cortical neurons are affected (and presumably damaged) by prolonged electrical stimulation, they absorb more of the histologic stain during subsequent processing, and become darker (hyperchromic). Also, they become less spherical and more irregularly shaped. Both of these changes can be quantified by the image analysis software. The staining density of the neurons is quantified as a light absorption ratio O =(Gc - Gm)/(Gn-Gm) where Gc is the average light level of the cell (neuron). With our CCD camera, the image light level ranges from 0 (darkest) to 255 (brightest) . Gm is the unattenuated light level and Gn is the light level of the neuropil from a part of the same histologic section, but from an area unaffected by the stimulation. For a CCD camera having a linear relation between light intensity and signal output (grey level), O is not affected by the intensity of the illumination, and since in our formulation of O, the amount of light absorbed by the cell is normalized on the amount absorbed by the neuropil, this index should not be strongly affected by the thickness of the

histologic sections or by the density of the staining. O is high for normal neurons and lower for darker (hyperchromic) neurons.

The change in the shape of the neurons can be quantified as A, the ratio of the long and short axis through the centroid (center of gravity) of the neuron's profile. A is a rather crude measure of the tendency of damaged neurons to become somewhat shriveled and elongated. Unlike the conventional measures of roundness, (circularity) the axis ratio does not require an accurate delineation of the perimeter of the cell (impossible when the contrast between the cell and the neuropil is low). However, the value of A will be affected by the mechanical flattening of the cell bodies that may occur when a microelectrode stretches the neuropil during insertion. Therefore, the neurons must be sampled from a region that does not manifest this type of distortion.

Figure 10 is a plot of A against O, for the normal cortical neurons from Figure 9A and also for the strongly affected neurons and moderately affected neurons shown in Figure 9B and 9C. Each symbol represents one neuron. The contribution of axis ratio and optical abortion ratio to each point can be combined into a single metric by computing $z=(O^2+A^2)^{½}$, the Euclidian distance of the point from the origin of the co-ordinate system formed by O and A. The z-values from the three populations can then be compared using standard statistical techniques, such as an analysis of variance :

Summary Table for analysis of variances of Z-vectors from normal vs. Strongly affected neurons (N=25)

Variable	Effect Size	Sum of Squares	df	Mean Square	F-Ratio	p
stim.effect	R = 0.77	0.55	1	0.27	232.92	< .0001
Error	0.39	023	.01			

Summary Table for analysis of variances of Z-vectors from normal and moderately affected neurons (N=25)

Variable	Effect Size	Sum of Squares	df	Mean Square	F-Ratio	p
stim.effect	R = 0.71	.024	1	0.24	22.92	< .0005
Error	0.24	023	.01			

Summary Table for Z-vectors from strongly and moderately affected neurons (N=23)

Variable	Effect Size	Sum of Squares	Df	Mean Square	F-Ratio	p
Stim.effect	R = 0.43	0.05	1	.05	4.69	<.04
Error	0.24	023	.01			

The analysis shows a highly significant difference between the z-vectors of the strongly affected and moderately affected neurons, vs. The normal neurons ($p < .0001$ and $p < .0005$, respectively, in the 2-sided tests). Furthermore, the neuronal populations that were judged by an experienced histopathologist to be moderately and strongly affected by the stimulation were found to be significantly different from each other in the statistical analysis of their morphometric data ($P < .04$). This significant difference was seen in spite of the small population of cells examined, as will be the case when the neurons close to the tip of a microelectrode are examined. Another useful parameter of the statistical analysis is the effect size (R) which quantifies the magnitude of the effect of the stimulation, relative to the variance of the z-vectors within each population. R was 0.77 for the contrast between the normal and severely affected cells, 0.71 for the contrast between the normal and moderately affected cells, and 0.43 for the contrast between the moderately and severely affected cells.

Figure 11 shows the site of the tip of a microelectrode from cat IC86. This chronically-implanted iridium mciroelectrode was pulsed for 7 hours with charge-balanced biphasic pulse pairs, 150 μsec/phase in duration (50 Hz, 60 μA, 9 nC/phase). The cat was sacrificed immediately after the end of the stimulation. The analysis of variance of the z-vectors of the neurons immediately beneath the site of the tip, vs the neurons from an unstimulated part of the cortex is given below:

Summary Table for Z-vectors from neurons near tip and neurons remote from the tip of electrode IC86-2 (N=24)

Variable	Effect Size	Sum of Squares	df	Mean Square	F- Ratio	p
stim.effect.	R = 0.28	0.02	1	0.02	1.81	.2
Error		0.29	22			

The z-vectors from the two population are not significantly different (p=0.2) and the effect size is small (R=0.28).This is consistent with our subjective evaluation that the electrical stimulation had no discernable effect on the neurons. However, the analysis does suggest the neurons subjacent to the tip may have slightly reduced z-values; there is a statistical "trend" that might reach significance if the data from many pulsed electrodes were to be pooled and compared with the neurons from unpulsed sites.

These preliminary data indicate that a morphometric analysis can add a useful dimension to our studies of stimulation-induced neuronal damage in the CNS, especially in situations requiring quantitation of changes in small populations of neurons, such as a dose-response study of the effect of microstimulation on the neurons surrounding the microelectrode's active site.

REFERENCES

Afifi, A.A. and Azen Statistical analysis, a Computer-oriented Approach Academic press, New York/London 1972.

Agnew, W.F. and McCreery, D.B., Yuen, T.G.H., and Bullara(1990) Local anesthetic block protects against electrically-induced damage in peripheral nerve J. Biomed. Eng. 12:301-308 .

Agnew, W.F. and McCreery, D.B., Bullara, L.A. and Yuen, T.G.H.: Effects of prolonged electrical stimulation of peripheral nerve. In: Neural Prostheses: Fundamental Studies, Agnew, W.F. and McCreery, D.B., eds., Prentice Hall, Englewood Cliffs, N.J., 1990.

Dyck. P.J. (1989) Does Hypoxia play a role in diabetic neurophathy? Neurology 111-118.

Kanda.T. (1984) Morphometric analysis of sural nerve in elderly diabetes mellitus. Bull Tokyo Med Dent Univ (JAPAN) 31 (4) p209-24.

Gorman, P.H. and Mortimer, J.T. (1983). The effect of stimulus parameters on the recruitment characteristics of direct nerve stimulation. IEEE Trans. Biomed. Eng., BME-30:7,407-414.

McCreery, D.B., Agnew, W.F., Yuen, T.G.H. and Bullara, L.A. (1992) Damage in peripheral nerve from continuous electrical stimulation: comparison of two stimulus waveforms. Med. & Biol. Eng. & Comput. 30:109-114.

McCreery, D.B., Agnew, W.F., Yuen, T.G.H. and Bullara, L.A. (1995) Relation between stimulus amplitude, stimulus frequency, and neural damaged during electrical stimultion of the sciatic nerve of the cat Med. & Biol. Eng. & Comput. 33:426-429.

Rattay,F. (1989). Analysis of models for extracellular fiber stimulation. IEEE Trans. Biomed. Engr 36:676-682.

Rubenstein,J.T.(1991) Analytical theory for extracellular stimulaion of nerve with focal electrodes II: Pasive myelinated axon Biophysics J 60:538-555 .

Torch, S. Usson, Y. And R.Saxod (1989) Automated Morphometric study of human peripheral nerve by image analysis Path. Res. Pract 185:567-571.

van der Honert, C. and Mortimer, J.T. (1979) The response of the myelinated nerve fiber to short duration biphasic stimulating currents. Ann. Biomed. Eng. 7:117-125.

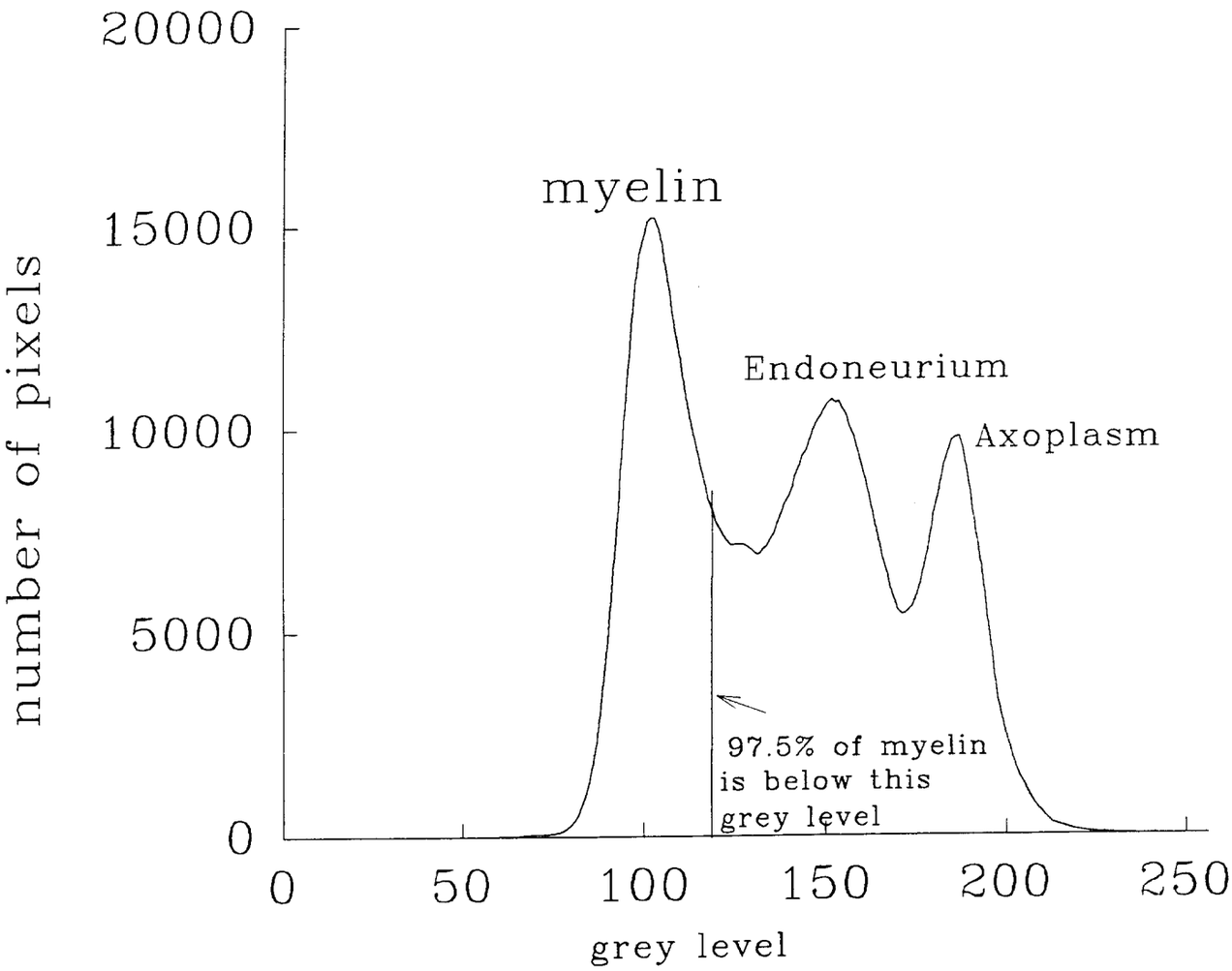
20000
15000
10000
5000
0
number of pixels
myelin
Endoneurium
Axoplasm
97.5% of myelin
is below this
grey level
0
50
100
150
200
250
grey level

Figure 1

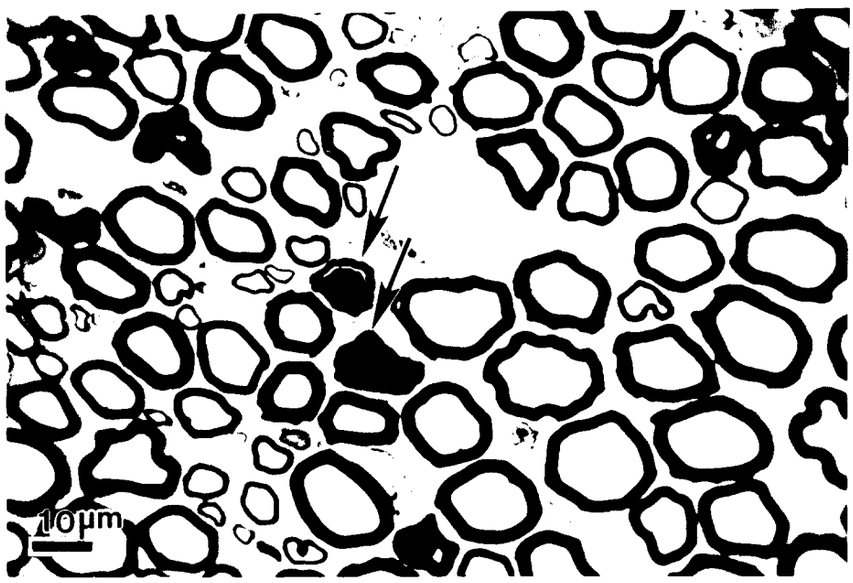

Figure 2A

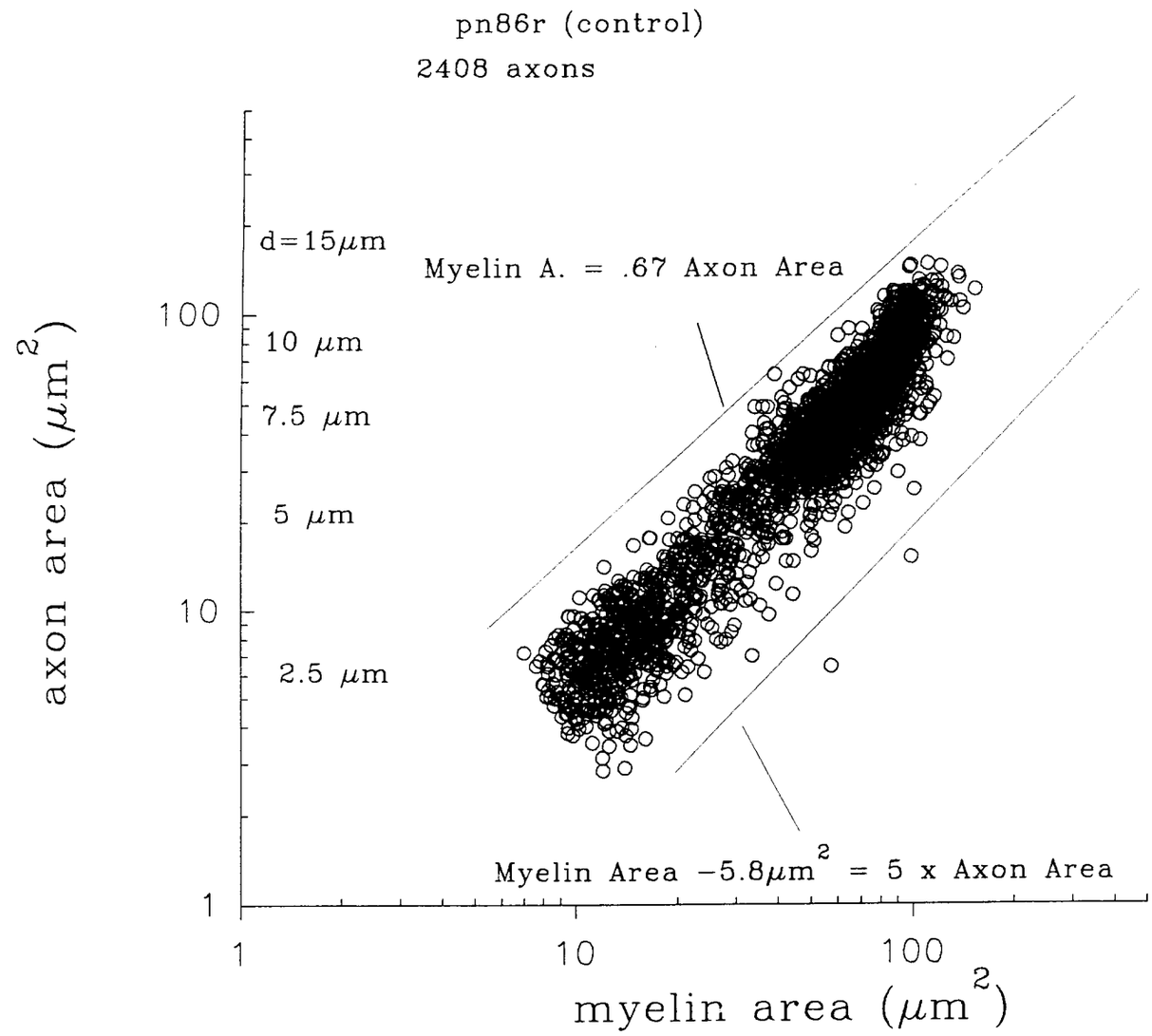

edc/pn86r/86rlogb1.spg

Figure 2B

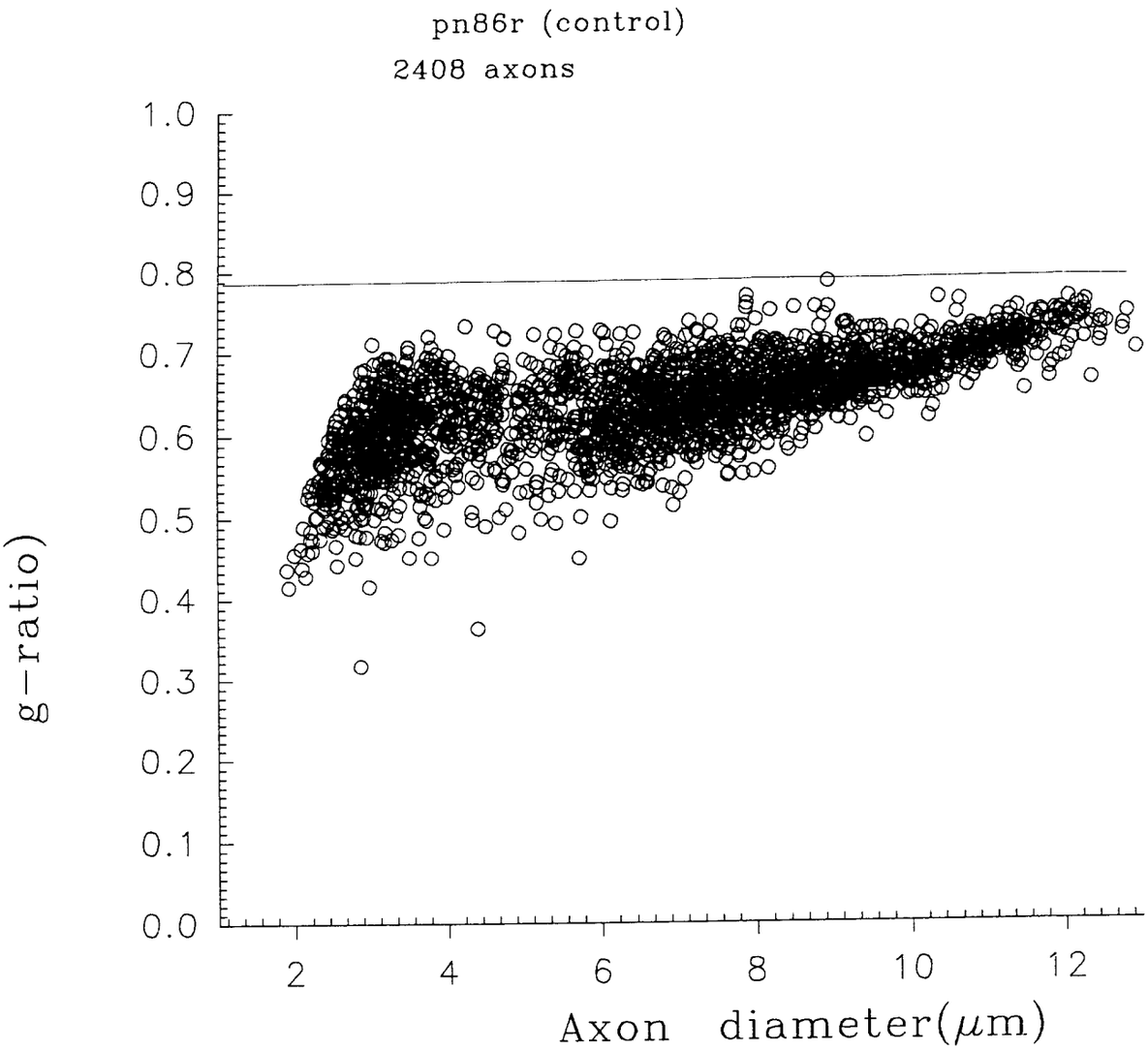

edc/pn86r/86r_g..spg

Figure 2C

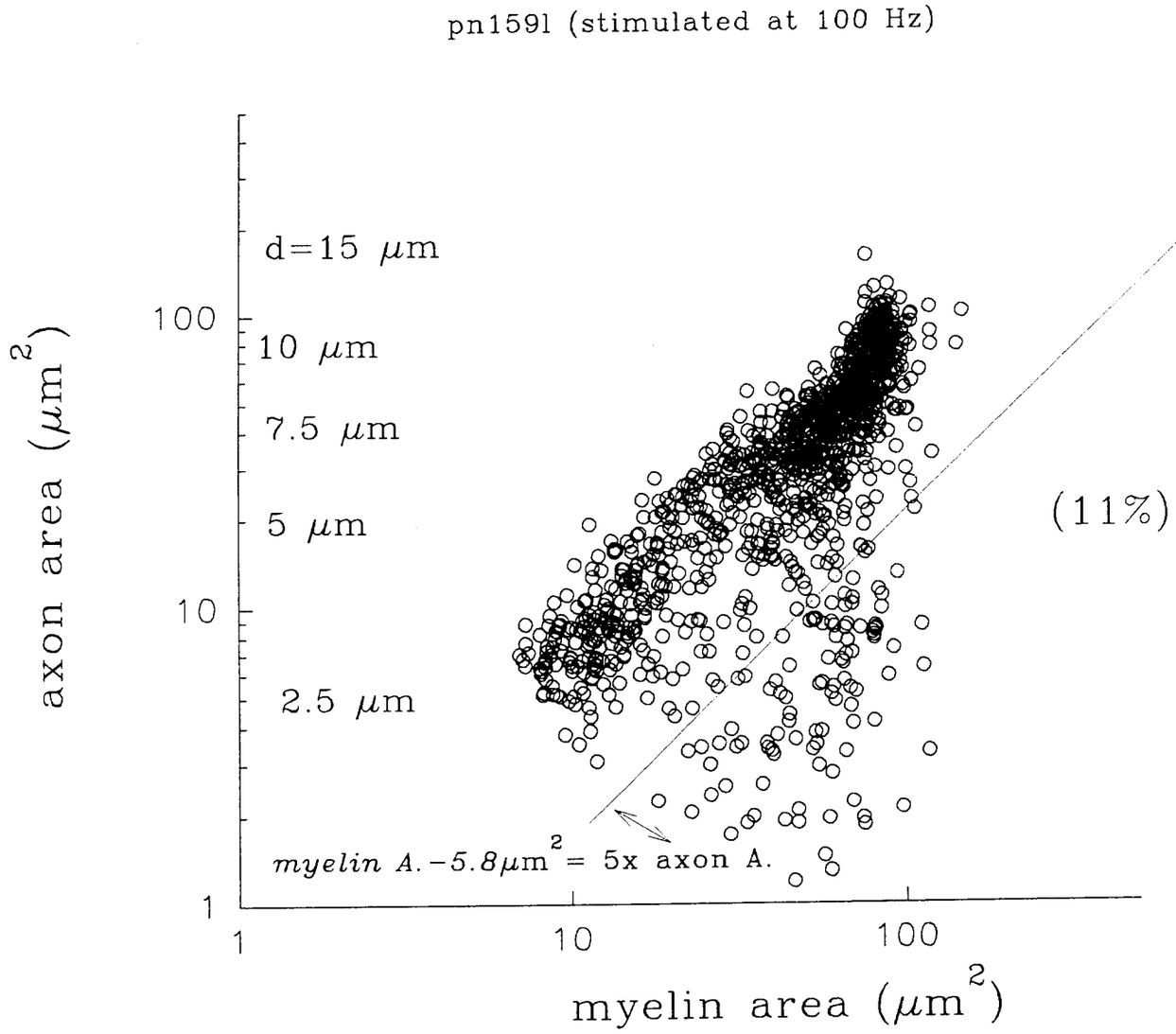

edc/pn1591/1591log1.spg

Figure 3A

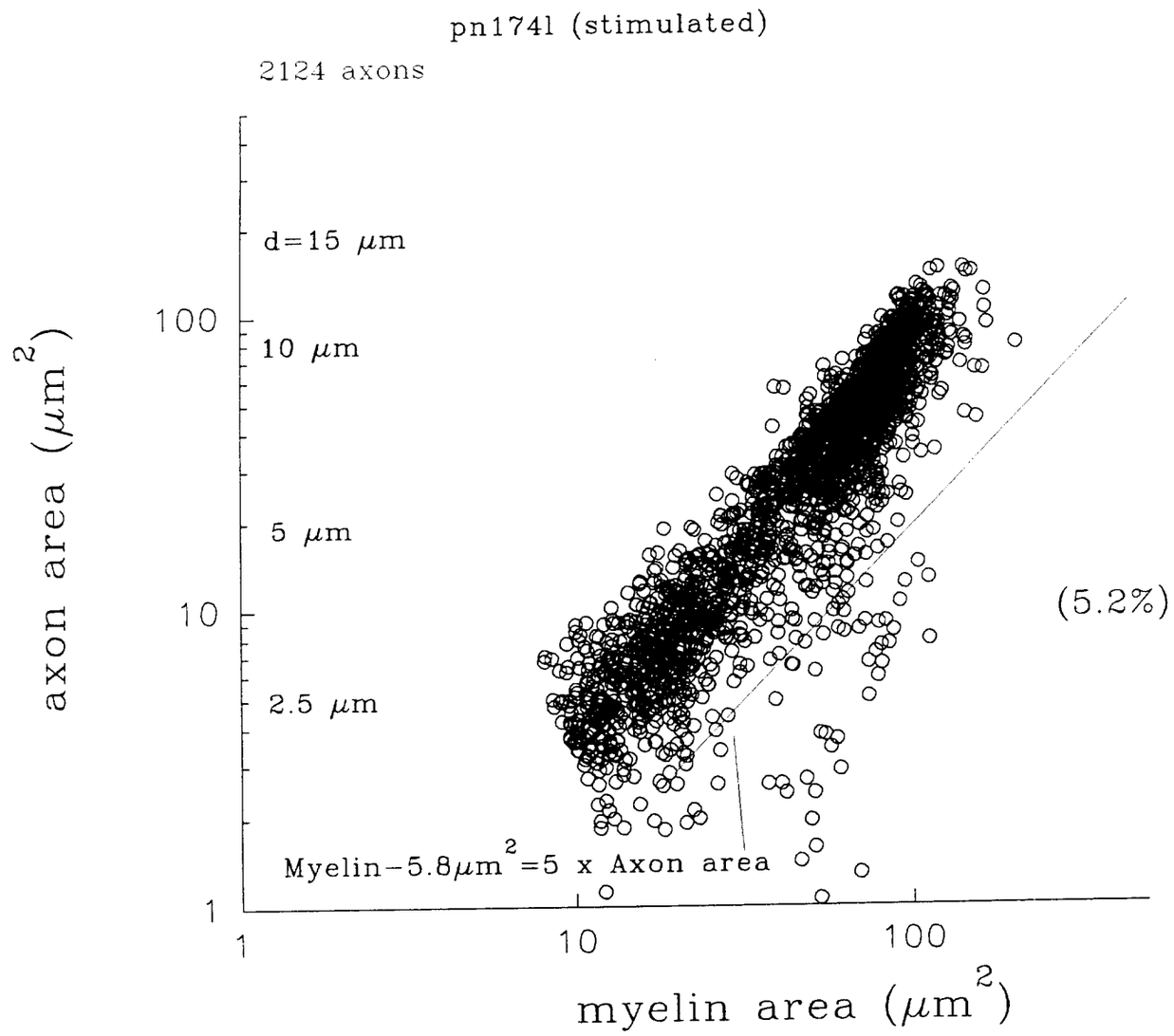

edc/pn1741/1741log1.spg

Figure 3B

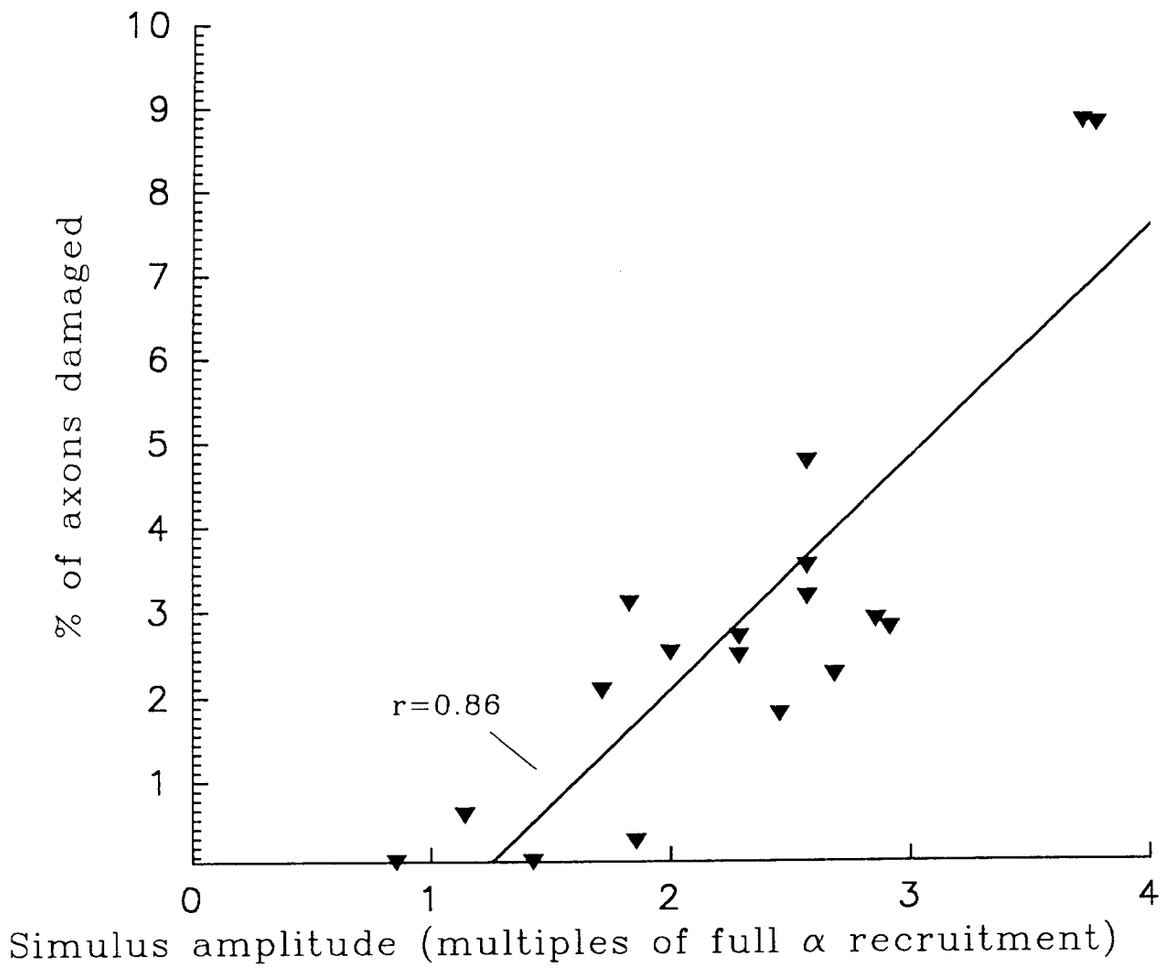

pn\newglu15.spg

Figure 4

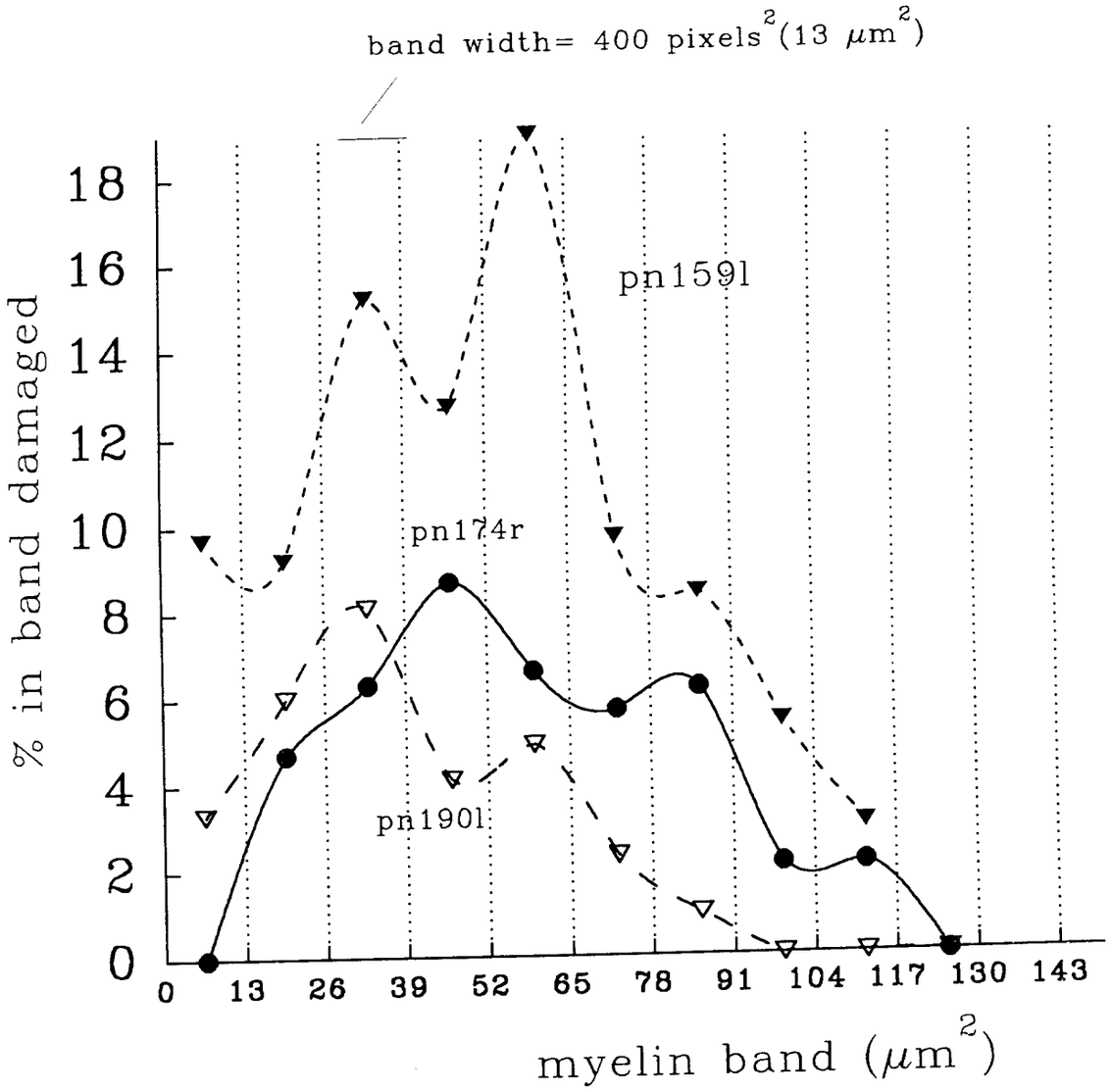

c;\plot41\pn\dambands.spg

Figure 5

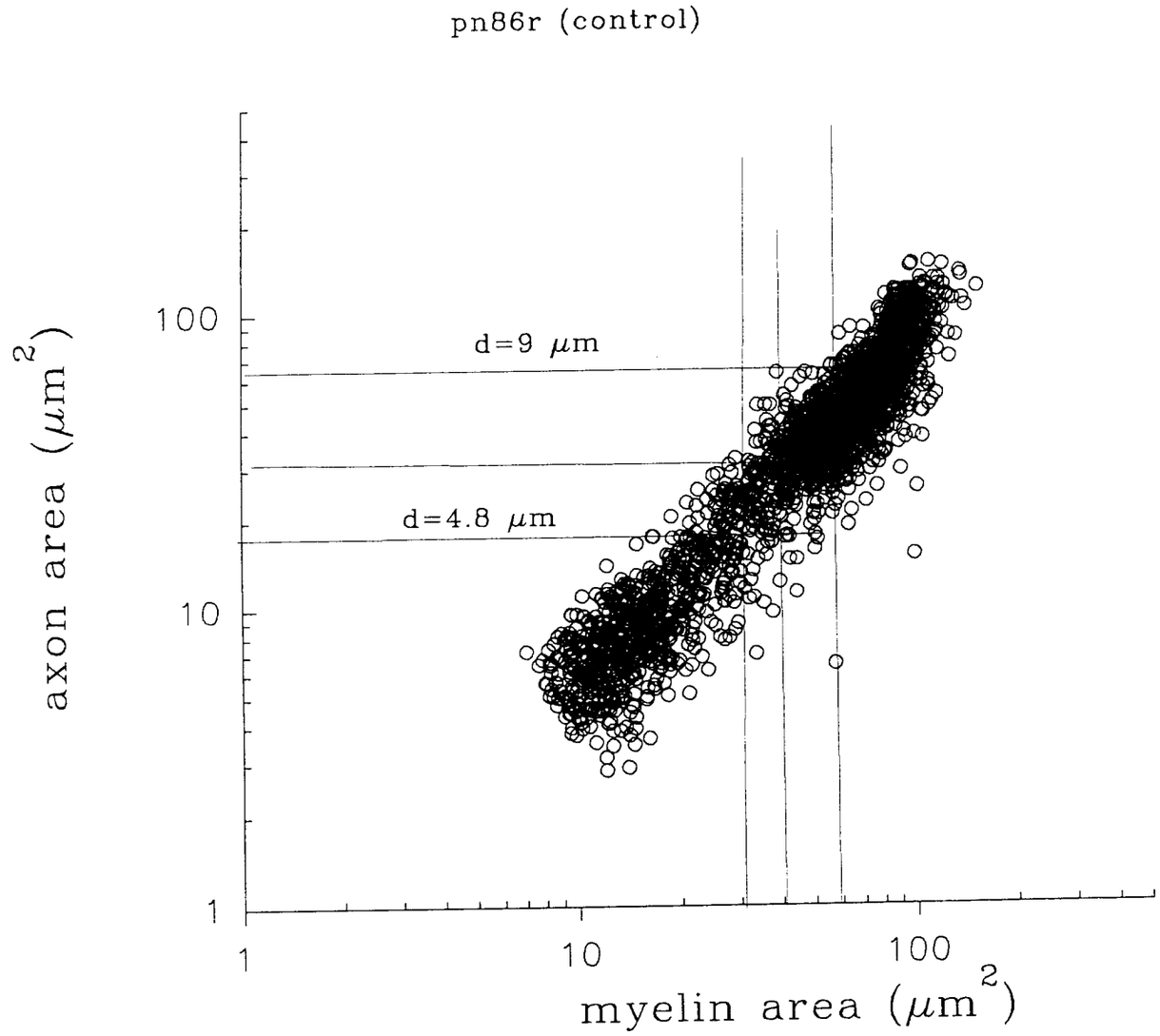

edc/pn86r/86rloge1.spg

Figure 6

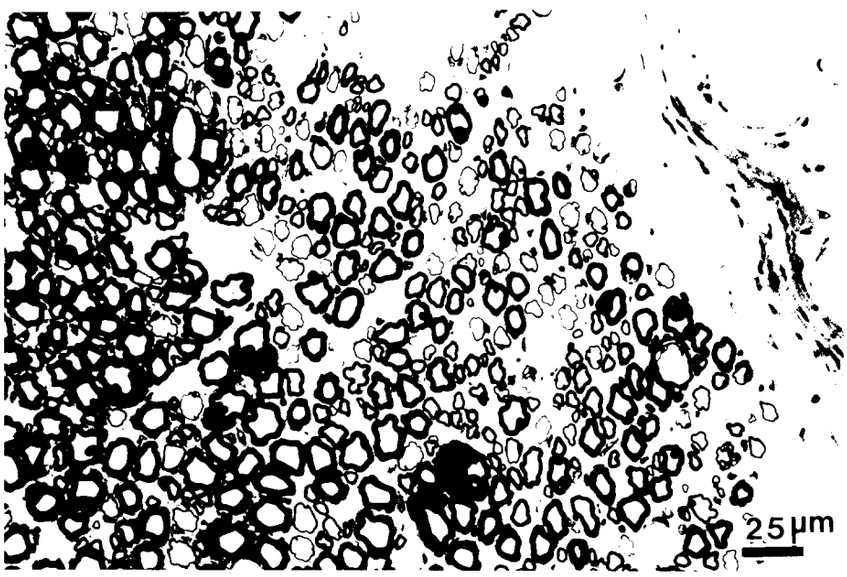

Figure 7A

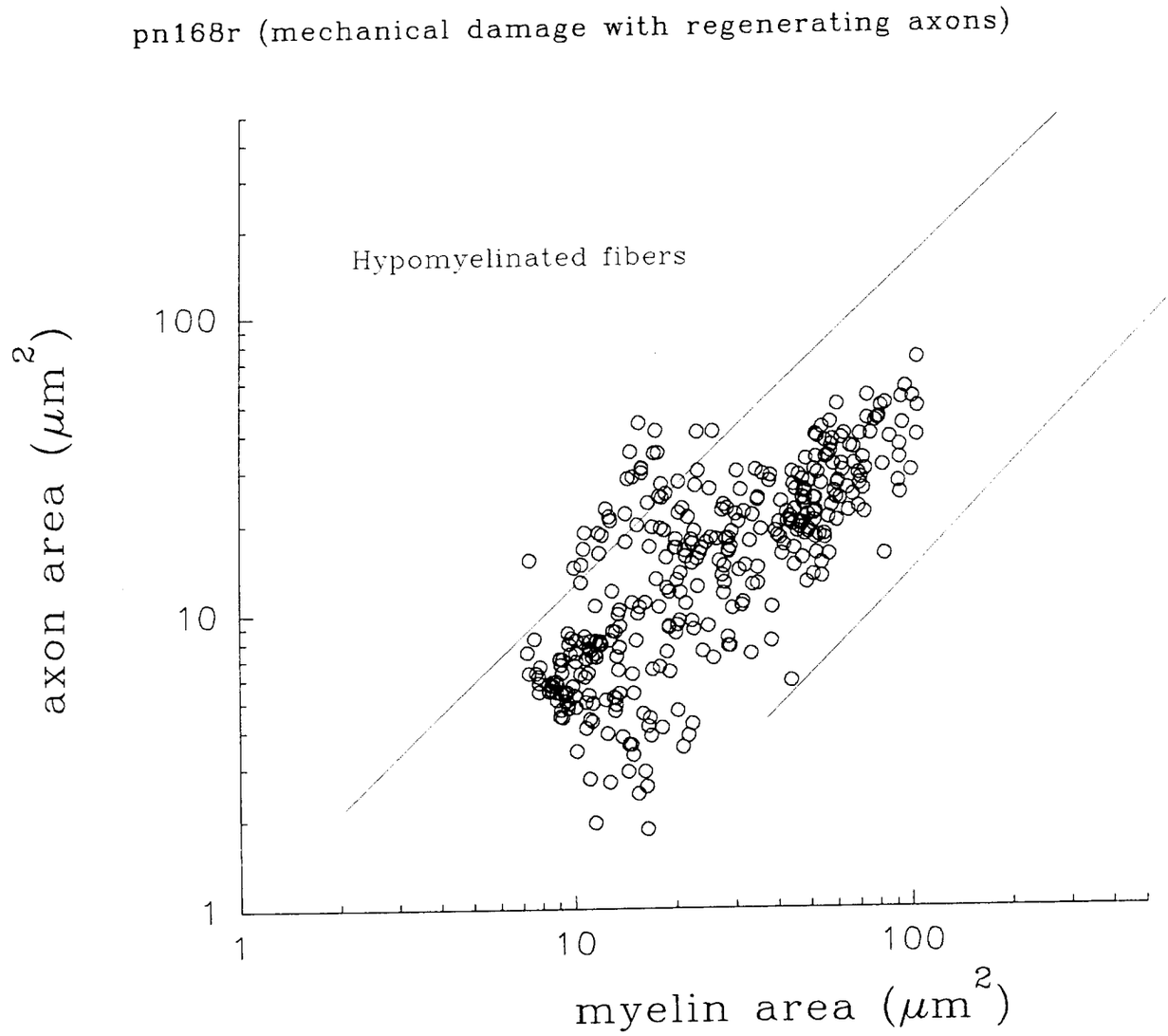
pn168r (mechanical damage with regenerating axons)
Hypomyelinated fibers
axon area (μm^2)
100
10
1
1
10
100
myelin area (μm^2)
d:\edc\mech168r/168rlog.spg

Figure 7B

pn192L (Sacrificed 5 weeks after stimulation)

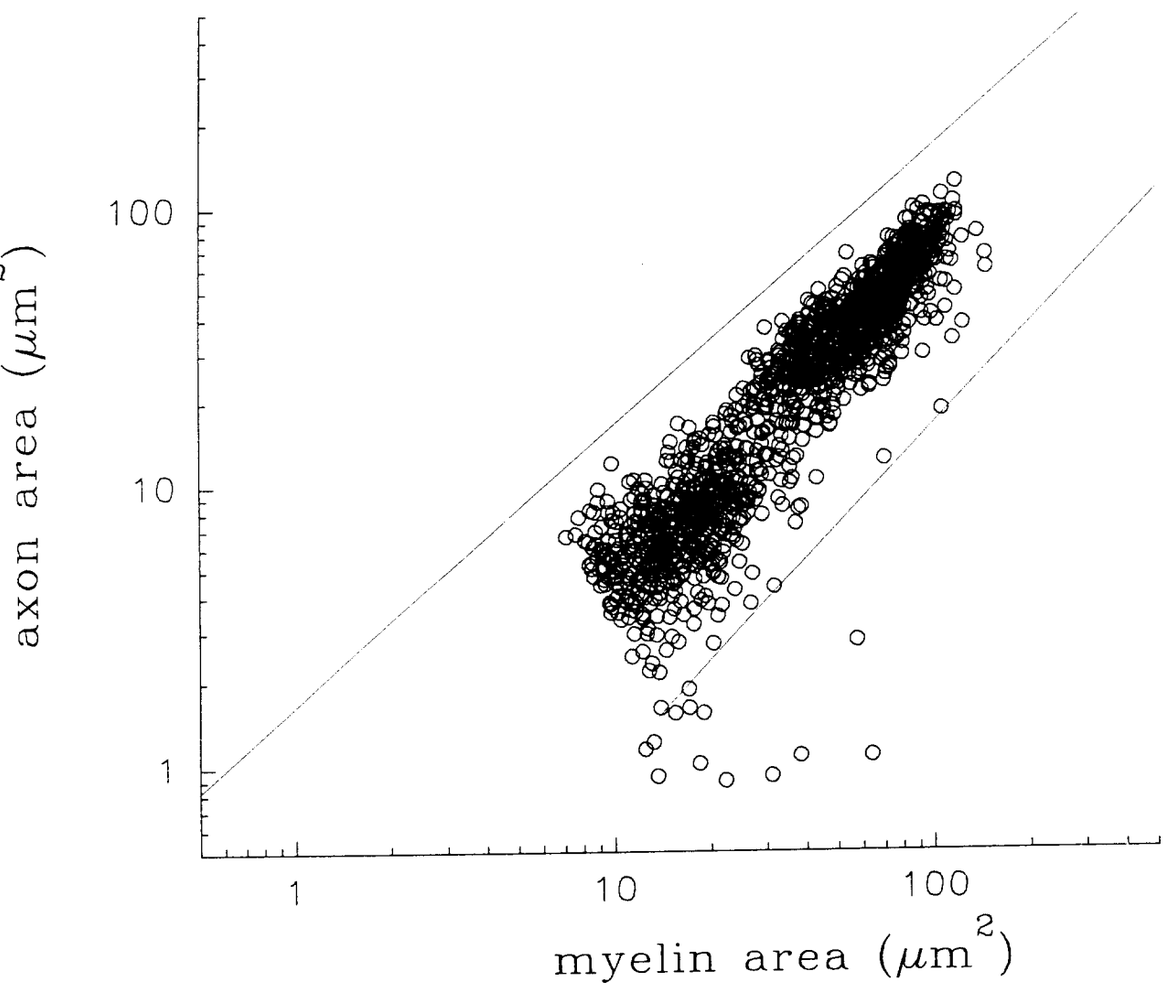

d:\pn192/192logc.spg

Figure 8A

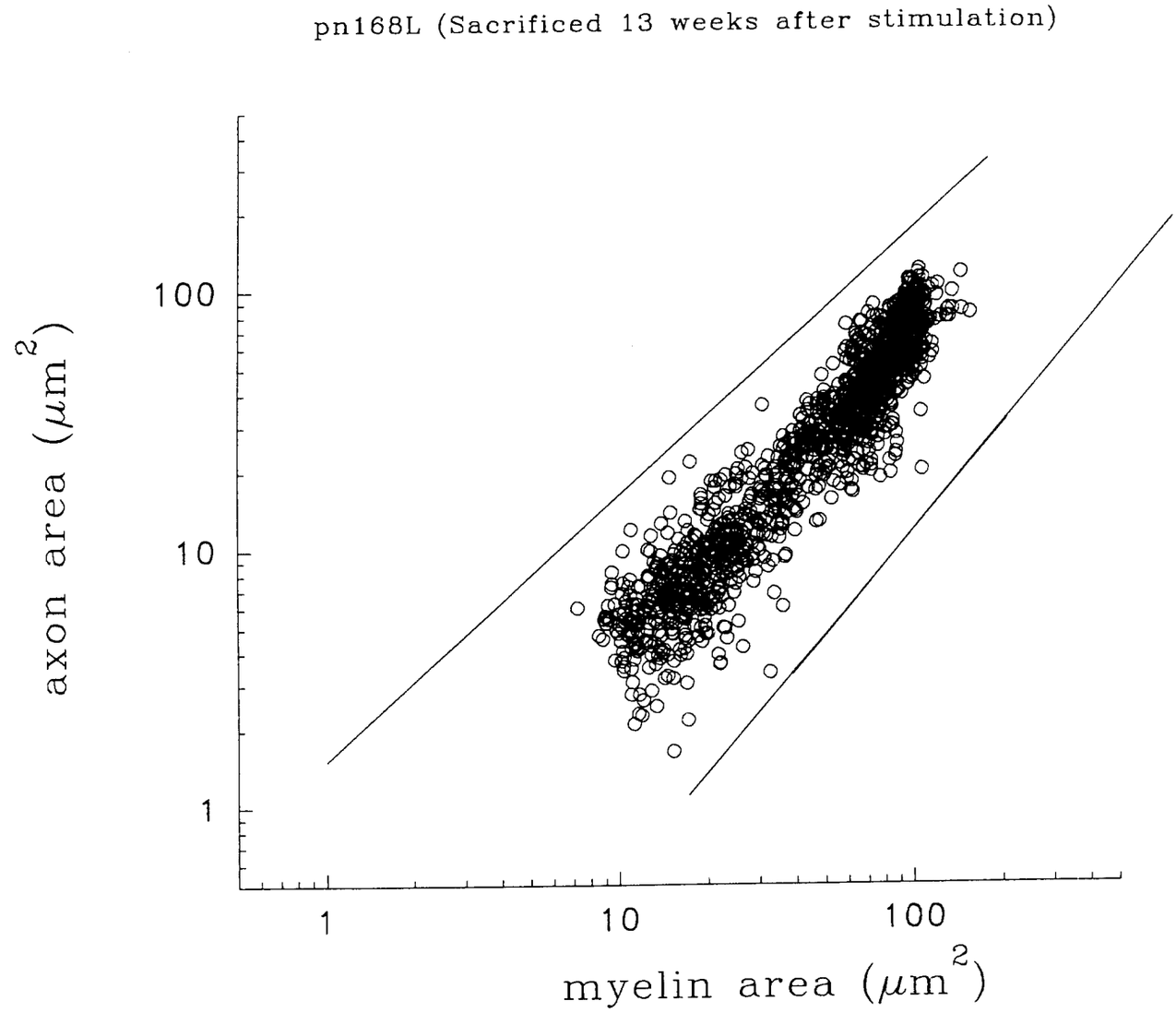

d:\pn168l/168llog1.spg

Figure 8B

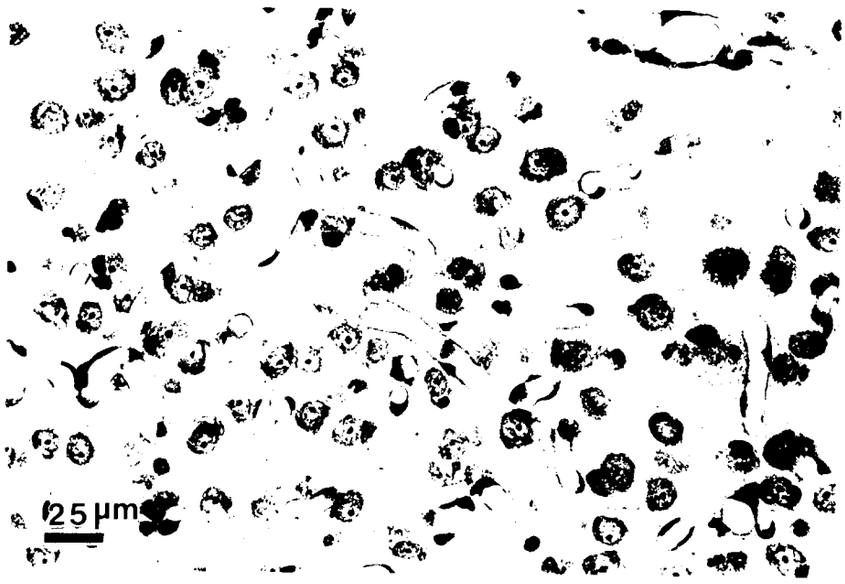

Figure 9A

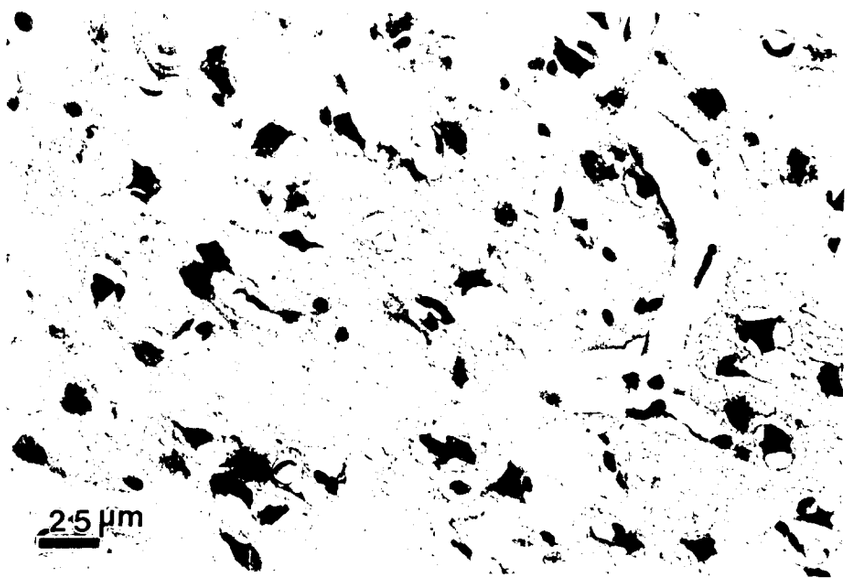

Figure 9B

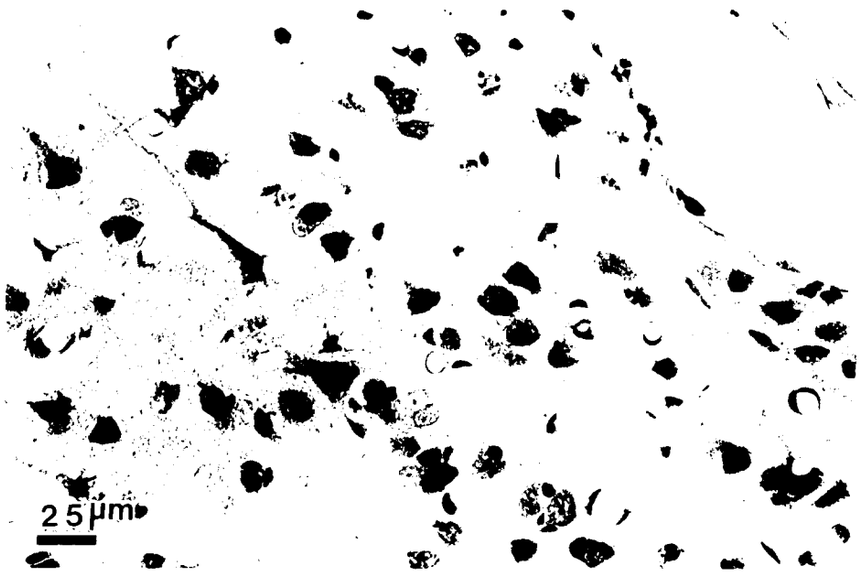

Figure 9C

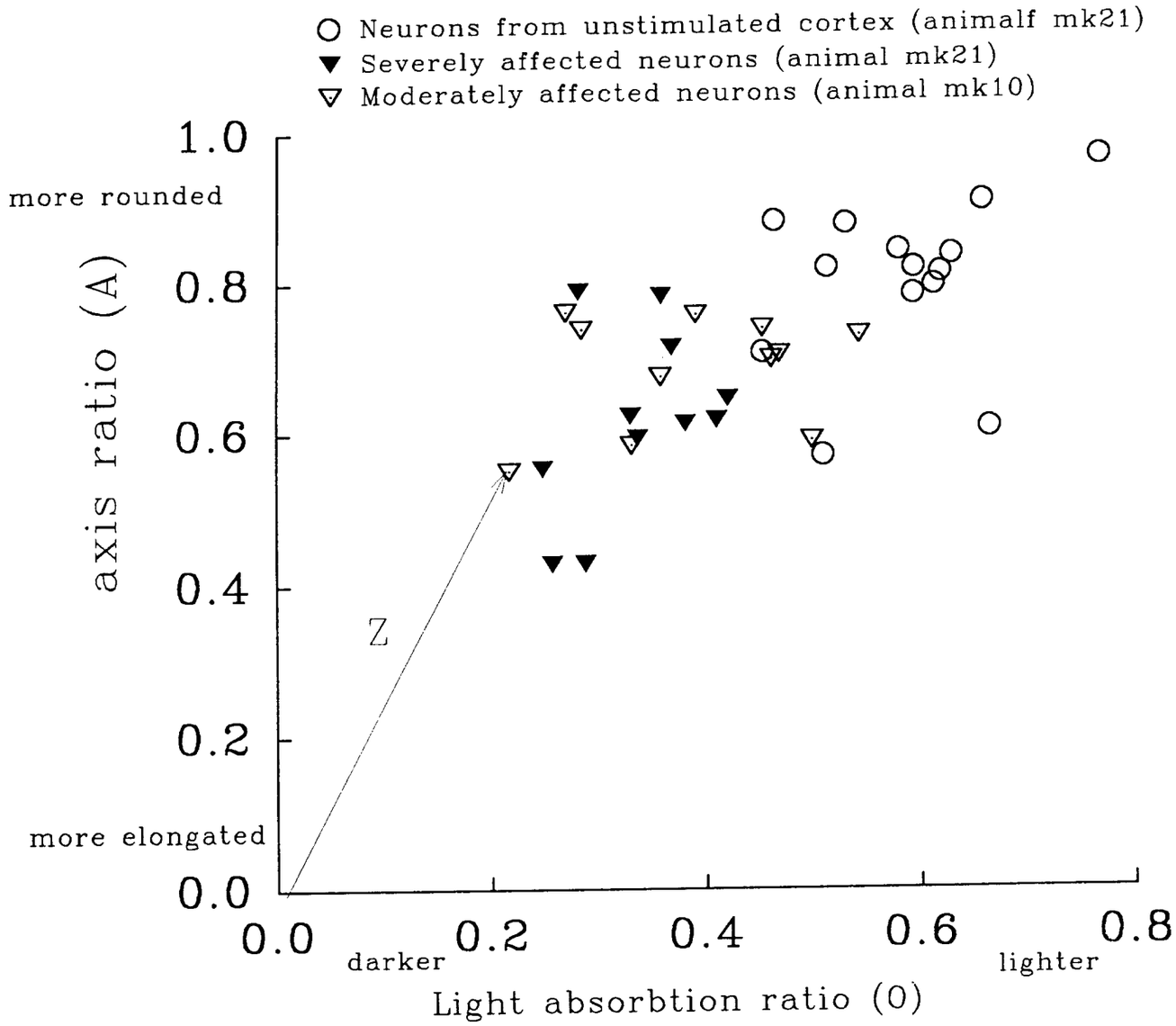

d:\edc\mk21sd\mk21b.spg

Figure 10

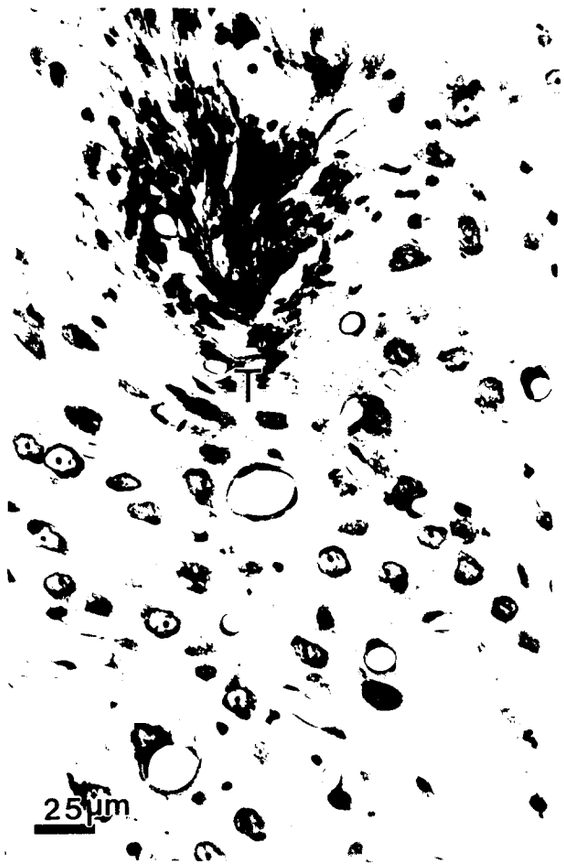

Figure 11

METHODS

Morphometric analysis of stimulation-induced injury in peripheral nerve.

The HMRI bidirectional helical stimulating electrode array was used in this study. The stimulating electrodes were implanted around both sciatic nerves of adult cats of either sex. A pair of recording electrodes is implanted subcutaneously over the lumbosacral spinal cord to record the compound action potentials evoked in the sciatic nerve by the stimulating electrode. One recording electrode is implanted at approximately the L5 level, and the other member of the pair is implanted approximately 5 cm caudally. With this arrangement, the compound action potentials evoked in the left or right nerve can be recorded with a single pair of recording electrodes, and there will be no danger of inflicting additional mechanical trauma upon the nerve or nerve roots.

Three weeks or more after implantation of the electrodes, the cats were anesthetized with Propofol and both nerves were stimulated continuously for 8 hours. The stimulus waveform was a charge-balanced, controlled-current, biphasic pulse pair. Each phase of the biphasic pair is 100 μsec in duration, with a 400 μsec delay between the first and second phases. This waveform excites both large and small axons in the nerve (Gorman and Mortimer 1983, McCreery et al 1992, van der Honert and Mortimer 1979).

Prior to the start of the 8 hours of continuous stimulation, we measured the recruitment characteristics of the Averaged evoked Compound Action Potential (AECAP), the response evoked by the stimulating electrodes and recorded over the spinal cord. In the peripheral nerve of the cat the first large component of the AECAP (the α component) represents the activity in the alpha and gamma efferent axons and the large afferent axons. To determine the recruitment characteristics of α component of the AECAP, the nerve is stimulated at each of several amplitudes, and the amplitude of the α component is plotted against the stimulus pulse amplitude. In addition, five unstimulated nerves were included in the study.

A

24

The sciatic nerves were prepared for histologic examination, as described in previous Quarterly reports and publications. The nerves were resected from the leg and embedded in plastic (Polysciences Polybed), cut to a thickness of 1 μm. The myelin was stained with osmium, and the endoneurium and axoplasm was counter-stained with methylene Blue.

For each nerve, 12 microscopic fields, each spanning approximately 186 x 180 μm, were scanned into the computer, using a high-resolution CCD camera (1024 x 972 pixels, and 256 grey levels). Each digitized image was then analyzed using a commercial image analysis program (Global Lab Image, from Data Translation, Inc). This program can identify objects within the field of the digitized image. For each field, the operator must specify a grey level (brightness), by which the GLI software establishes the boundary between the object and the surrounding background. The histograms of the grey levels of the approximately 1,000,000 pixels forming the image is computed by the GLI software, and then analyzed by a custom software utility. The histogram contains 3 peaks, representing the myelin (darkest), the endoneurium surround the myelin, (lighter) and the axoplasm (lightest). A typical histogram is shown in Figure 1. The custom software deconvolves the peaks, and identifies the grey level that is brighter than 97.5% of the myelin. This grey level is then used to obtain the optimal differentiation between the myelin and the surrounding endoneurium.

Eleven morphometric parameters were computed for each object, including total area, area of included holes, roundness (circularity) and average brightness. The tabulated parameter files were then edited and analyzed with the aid of a custom software program in order to remove artifact objects and joined objects, and all objects having a total cross sectional area less than 10 μm^2 (small myelinated axons cannot be identified reliably by the image analysis program, due to their low and variable contrast against the surrounding endoneurium).The number of fibers undergoing early axonal degeneration was also counted automatically, using criteria established from the morphometric analysis of unstimulated nerves.

METHODS

Morphometric analysis of stimulation-induced injury in peripheral nerve.

The HMRI bidirectional helical stimulating electrode array was used in this study. The stimulating electrodes were implanted around both sciatic nerves of adult cats of either sex. A pair of recording electrodes is implanted subcutaneously over the lumbosacral spinal cord to record the compound action potentials evoked in the sciatic nerve by the stimulating electrode. One recording electrode is implanted at approximately the L5 level, and the other member of the pair is implanted approximately 5 cm caudally. With this arrangement, the compound action potentials evoked in the left or right nerve can be recorded with a single pair of recording electrodes, and there will be no danger of inflicting additional mechanical trauma upon the nerve or nerve roots.

Three weeks or more after implantation of the electrodes, the cats were anesthetized with Propofol and both nerves were stimulated continuously for 8 hours. The stimulus waveform was a charge-balanced, controlled-current, biphasic pulse pair. Each phase of the biphasic pair is 100 μsec in duration, with a 400 μsec delay between the first and second phases. This waveform excites both large and small axons in the nerve (Gorman and Mortimer 1983, McCreery et al 1992, van der Honert and Mortimer 1979).

Prior to the start of the 8 hours of continuous stimulation, we measured the recruitment characteristics of the Averaged evoked Compound Action Potential (AECAP), the response evoked by the stimulating electrodes and recorded over the spinal cord. In the peripheral nerve of the cat the first large component of the AECAP (the α component) represents the activity in the alpha and gamma efferent axons and the large afferent axons. To determine the recruitment characteristics of α component of the AECAP, the nerve is stimulated at each of several amplitudes, and the amplitude of the α component is plotted against the stimulus pulse amplitude. In addition, five unstimulated nerves were included in the study.

The sciatic nerves were prepared for histologic examination, as described in previous Quarterly reports and publications. The nerves were resected from the leg and embedded in plastic (Polysciences Polybed), cut to a thickness of 1 μm. The myelin was stained with osmium, and the endoneurium and axoplasm was counter-stained with methylene Blue.

For each nerve, 12 microscopic fields, each spanning approximately 186 x 180 μm, were scanned into the computer, using a high-resolution CCD camera (1024 x 972 pixels, and 256 grey levels). Each digitized image was then analyzed using a commercial image analysis program (Global Lab Image, from Data Translation, Inc). This program can identify objects within the field of the digitized image. For each field, the operator must specify a grey level (brightness), by which the GLI software establishes the boundary between the object and the surrounding background. The histograms of the grey levels of the approximately 1,000,000 pixels forming the image is computed by the GLI software, and then analyzed by a custom software utility. The histogram contains 3 peaks, representing the myelin (darkest), the endoneurium surround the myelin, (lighter) and the axoplasm (lightest). A typical histogram is shown in Figure 1. The custom software deconvolves the peaks, and identifies the grey level that is brighter than 97.5% of the myelin. This grey level is then used to obtain the optimal differentiation between the myelin and the surrounding endoneurium.

Eleven morphometric parameters were computed for each object, including total area, area of included holes, roundness (circularity) and average brightness. The tabulated parameter files were then edited and analyzed with the aid of a custom software program in order to remove artifact objects and joined objects, and all objects having a total cross sectional area less than 10 μm^2 (small myelinated axons cannot be identified reliably by the image analysis program, due to their low and variable contrast against the surrounding endoneurium).The number of fibers undergoing early axonal degeneration was also counted automatically, using criteria established from the morphometric analysis of unstimulated nerves.